the aromatic compounds was controlled by the reservoir temperature and an adjustable needle valve. The forward power was measured by a built-in wattmeter. Reflected power was ajusted by two variable capacitors to less than 5% of the forward power. Mixing took place before the reactants entered the plasma zone. The pressure was about 0.5 Torr. Flow rates were determined by the amount of material lost from the reactant container and the time of plasmolysis. Products and unreacted starting materials were frozen out in a liquid nitrogen cooled trap which was located immediately beyond the plasma zone. The glowing plasma zone was typtically about the same length as the coil, i.e., 15 cm. In general, only a small amount of polymeric film was produced on the wall of the reactor tube. This contrasts strongly with the large amounts of polymer from cyanogen alone or benzene alone.

Analysis. Analysis of products were carried out by temperature-programmed GLC. A 6-m 20% β,β-oxydipropionitrile column was used for cyanogen and gaseous products. Aromatic products were analyzed by a 4-m 10% Carbowax 20M column or a 3-m 10% silicone SE 30 column. The products were identified by comparison with authentic samples and in most cases confirmed by GLC–MS. Yields were estimated by GLC with an internal standard. Hydrogen cyanide was determined by silver nitrate precipitation titration. Products which did not elute from the GLC were not investigated.

Acknowledgment. This work was supported by the National Science Foundation. We thank Mr. J. Hovelsrud for technical assistance.

High Resolution, Zero Quantum Transition (Two-Dimensional) Nuclear Magnetic Resonance Spectroscopy: Spectral Analysis

G. Pouzard,[1] S. Sukumar, and L. D. Hall*

Contribution from the Department of Chemistry, University of British Columbia, Vancouver, British Columbia, Canada V6T 1Y6. *Received September 6, 1980*

Abstract: The explicit analysis of zero quantum transition (ZQT) NMR spectra is given for weakly coupled homonuclear spin $^1/_2$ systems (AB, ABC, ABCD, . . .); used in conjunction with conventional single quantum transition (SQT) spectra, they provide a more complete description of the spin system concerned. ZQT spectral analysis for a typical organic molecule is demonstrated with the use of trideuteriomethyl 2,3,4,6-tetra-*O*-(trideuterioacetyl)-α-D-glucopyranoside as an example.

Introduction

The advent of two-dimensional (2D) nuclear magnetic resonance (NMR) spectroscopy[2-7] has opened many new horizons for the practicing spectroscopist and chemist alike. One of the more exciting new opportunities associated with this technique is the possibility of observing transitions for weakly coupled spin systems which would otherwise be "forbidden", such as combination lines or multiple quantum transitions.[8,9] For example, it has recently been demonstrated that zero and multiple quantum transitions (ZQT and MQT) of simple spin systems can be selectively detected[8,10] or, even excited.[11]

Study of ZQT spectra, and their explicit analysis, is of particular interest for many reasons; thus, such spectra can provide additional information on the spin system of interest which does not appear in the conventional single quantum transition (SQT) spectrum. ZQT spectra generally exhibit fewer lines than either conventional SQT spectra[9] or 2D chemical shift correlated spectra[12,13] and, furthermore, the widths of the resulting lines are independent of magnetic field inhomogeneity effects. Perhaps the most appealing feature for the practicing chemist is that all of the frequency information encoded in a ZQT spectrum is correlated via *differences* in both chemical shifts and coupling constants; the latter includes information concerning the relative signs of coupling constants. As we shall now show, these features can be recognized in the ZQT proton spectra of complex organic molecules and provide a potentially useful method for assigning the resonances of a conventional spectrum.

Although the properties of MQT spectra (more specifically, those involving double quantum transitions) have been described previously,[14,15] no explicit analysis of ZQT spectra has appeared

Table I. Energy Level Representation and the Possible *n*-Quantum Transition Frequencies for a Weakly Coupled AB Spin $^1/_2$ System

M	level	energy[a]	ΔM	transition	frequency
−1	4 − −	$(f_A + f_B)/2 + J/4$	0	2 → 3	$f_A - f_B$
0	3 − +	$(f_A - f_B)/2 - J/4$	1	1 → 2	$f_B - J/2$
0	2 + −	$-(f_A - f_B)/2 - J/4$	1	3 → 4	$f_B + J/2$
			1	1 → 3	$f_A - J/2$
+1	1 + +	$-(f_A + f_B)/2 + J/4$	1	2 → 4	$f_A + J/2$
			2	1 → 4	$f_A + f_B$

[a] Expressed in frequency units.

(1) On leave from University of Provence, St. Jerome, 13397 Marseille, Cedex 4, France.
(2) Jeener, J. Ampere International Summer School, Basko Polje, Yugoslavia, 1971 (unpublished).
(3) Aue, W. P.; Bartholdi, E.; Ernst, R. R. *J. Chem. Phys.* **1976**, *64*, 2229.
(4) Alla, M.; Lippmaa, E. *Chem. Phys. Lett.* **1976**, *37*, 260.
(5) Hester, R. K.; Akerman, J. L.; Neff, B. L.; Waugh, J. S. *Phys. Rev. Lett.* **1976**, *36*, 1081.
(6) Vega, S.; Shattuk, T. W.; Pines, A. *Phys. Rev. Lett.* **1976**, *37*, 43.
(7) Bodenhausen, G.; Freeman, R.; Niedermeyer, R.; Turner, D. L. *J. Magn. Reson.* **1977**, *26*, 133.
(8) Wokaun, A.; Ernst, R. R. *Chem. Phys. Lett.* **1977**, *52*, 407.
(9) Wokaun, A.; Ernst, R. R. *Mol. Phys.* **1978**, *36*, 317.
(10) Bodenhausen, G.; Vold, R. L.; Vold, R. R. *J. Magn. Reson.* **1980**, *37*, 93.
(11) Warren, W. S.; Sinton, S.; Weitekamp, D. P.; Pines, A. *Phys. Rev. Lett.* **1979**, *43*, 1791.
(12) Nagayama, K.; Wuthrich, K.; Ernst, R. R. *Biochem. Biophys. Res. Commun.* **1979**, *90*, 305.
(13) Bain, A. D.; Bell, R. A.; Everett, J. R.; Hugues, D. W. *J. Chem. Soc., Chem. Commun.* **1980**, 256.

0002-7863/81/1503-4209$01.25/0 © 1981 American Chemical Society

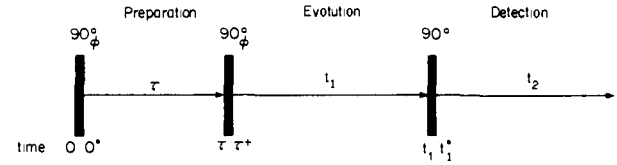

Figure 1. The basic pulse sequence for creation and detection of n-quantum transition spectra. The phase ϕ of the "excitation" pulses can be varied for selective detection of ZQT spectra (see text). The notation on the time scale is used in Table II.

in the literature. Because it should be of general interest, we now present that analysis for spin $^1/_2$ nuclides and demonstrate how it can be applied, in the form of a type of subspectral analysis, to a more complex spin system. It is appropriate to preface that analysis with a brief reminder of how ZQT (or MQT) are created and observed in a multiple pulse Fourier transform (FT) experiment.

Most NMR experiments involve single quantum transitions and can be simply understood in terms of the effect of pulses on classical magnetization vectors and subsequent precession (and relaxation) of these vectors in the rotating frame of reference. In contrast, ZQT (and MQT) cannot be visualized in the same sense, mainly because they are not observed directly in an FT experiment, and their creation and detection are best explained using the density matrix formalism, as summarized in the next section.

Creation and Observation of ZQT's in Pulsed NMR

The two-spin ($^1/_2$) system can be conveniently represented as a 4 × 4 matrix (σ) written in the eigenbasis of the Zeeman Hamiltonian (and F_z) (i.e., ++, +−, −+, −−); Table I gives the energy levels and all the possible transition frequencies for the AB case. The effect of a strong radio-frequency (rf) pulse of angle θ applied along the x asis of the rotating frame of reference can be described by the rotation operation which transforms the matrix σ into $[\sigma]_+$ such that

$$[\sigma]_+ = \exp(-i\theta F_x)\sigma \exp(i\theta F_x) \quad (1)$$

where the angular momentum operator projection $F_x = F_x^A + F_x^B$. Expanding the exponential form of the rotation operator yields explicit expressions for the elements of the new matrix $[\sigma]_+$.[16] It should be noted, however, that the new elements will also depend on the phase, ϕ, of the rf pulses, and hence the rotation operator should be written for a general case as

$$R(\theta,\phi) = \exp(-i\phi F_z) \exp(i\theta F_x) \exp(i\phi F_z) \quad (2)$$

For the present arguments a zero pulse phase (along the x axis) is assumed for convenience, but it will be noted later that for selective detection of n-quantum transitions it will be necessary to vary the phase, ϕ, of the rf "excitation" pulses[8,10,17] (Figure 1).

The NMR observable along the y axis of the rotating frame is given by

$$\langle M_y \rangle = \tfrac{1}{2}[(\sigma_{12} - \sigma_{21}) + (\sigma_{13} - \sigma_{31}) + (\sigma_{24} - \sigma_{42}) + (\sigma_{34} - \sigma_{43})]_+ \quad (3)$$

indicating that the detected signal contains only SQC's of the density matrix. However, the ZQT information is contained in the nondiagonal ZQC's of the density matrix; thus to detect ZQT (or MQT) spectra it is not only necessary to create ZQC's (or the MQ equivalent), but that information has to be transferred into the observable SQT by means of suitable pulse sequences.[8,18] Of the methods available for creation and detection of ZQC's,[8,18a-21] the pulse sequence shown in Figure 1 has proven to be both convenient and of general applicability and will be described here on a weakly coupled AB spin $^1/_2$ system.

Table II. σ_{12} and σ_{23} Elements of the (4 × 4) Density Matrix of an AB System, Following the Pulse Sequence shown in Figure 1[a]

time	expressions for the matrix elements, σ_{12} and σ_{23}
0[b]	$[\sigma_{12}]_0 = 0$ $[\sigma_{23}]_0 = 0$
0+	$[\sigma_{12}]_{0+} = i[(\sigma_{11} - \sigma_{22}) + (\sigma_{33} - \sigma_{44})]_0/4 = i\Delta P/2$[c] $[\sigma_{23}]_{0+} = 0$
τ	$[\sigma_{12}]_\tau = [\sigma_{12}]_{0+} \exp(-i\omega_{12}\tau) = i\Delta P\{\exp(-i)(\omega_B - J'/2)\tau\}/2$ $[\sigma_{23}]_\tau = [\sigma_{23}]_{0+} \exp(-i\omega_{23}\tau) = 0$
τ^+	$[\sigma_{12}]_{\tau^+} = [(\sigma_{12} + \sigma_{21}) + (\sigma_{34} + \sigma_{43}) - (\sigma_{13} - \sigma_{31}) + (\sigma_{24} - \sigma_{42})]_\tau/4$ $= \Delta P\{\sin(\omega_B\tau/2) \cos(J'\tau/2) + i \sin(\omega_A\tau/2)\, i \sin(J'\tau/2)\}/2$ $[\sigma_{23}]_{\tau^+} = i[(\sigma_{12} + \sigma_{21}) - (\sigma_{34} + \sigma_{43}) - (\sigma_{13} + \sigma_{31}) + (\sigma_{24} + \sigma_{42})]_\tau/4$ $= i\Delta P\{\sin(J'\tau/2) \sin((\omega_A + \omega_B)\tau/2) \cdot \sin((\omega_A - \omega_B)\tau/2)\}$
t_1	$[\sigma_{12}]_{t_1} = [\sigma_{12}]_{\tau^+} \exp(-i\omega_{12}t_1)$ $= \Delta P\{\sin(\omega_B\tau/2) \cos(J'\tau/2) + i \sin(\omega_A\tau/2)\, i \sin(J'\tau/2) \exp(-i\omega_{12}t_1)\}/2$ $[\sigma_{23}]_{t_1} = [\sigma_{23}]_{\tau^+} \exp(-i\omega_{23}t_1)$ $= i\Delta P\{\sin(J'\tau/2) \sin((\omega_A + \omega_B)\tau/2) \cdot \sin((\omega_A - \omega_B)\tau/2) \exp(-i\omega_{23}t_1)\}$
$t_1{}^{+d}$	$[\sigma_{12}]_{t_1{}^+} = \{[(\sigma_{12} + \sigma_{21}) + (\sigma_{34} + \sigma_{43}) - (\sigma_{13} + \sigma_{31}) + (\sigma_{24} - \sigma_{42})]_{t_1} + i[(\sigma_{14} - \sigma_{41}) + (\sigma_{23} - \sigma_{32})]_{t_1}\}/4$
t_2	$[\sigma_{12}]_{t_2} = [\sigma_{12}]_{t_1{}^+} \exp(-i\omega_{12}t_2)$[e]

[a] Energies are expressed in terms of angular velocities ω ($=2\pi f$) and J' ($=2\pi J$). The relaxation (T_2) terms have been omitted for convenience (see text). [b] Boltzmann equilibrium state. [c] $\Delta P = [(\sigma_{11} - \sigma_{22})]_0 = [(\sigma_{33} - \sigma_{44})]_0$. [d] At this stage it is only necessary to know the explicit form of the observable. [e] Form of the detected signal.

In order to understand the creation and detection of ZQC's, one can express just two elements, σ_{12}(SQC) and σ_{23}(ZQC), of the density matrix and follow the consequences of the rf pulses and the evolution of those matrix elements at various stages of the pulse sequence (Table II).

The initial (Boltzmann) state of the density matrix contains only the diagonal elements (σ_{nn}) corresponding to the equilibrium populations. The initial 90° pulse equalizes all diagonal elements and creates only SQC, and no ZQC (or MQC), as indicated by the $[\sigma]_{0+}$ elements in Table II; the explicit expressions for the corresponding elements may be derived from eq 1.[16] The nondiagonal SQC's, when allowed to develop during the preparation period τ, give elements of the form

$$\sigma_{nm}(\tau) = \sigma_{nm}(0^+) \exp(-i\omega_{nm}\tau) \exp(-\tau/T_{2nm}) \quad (4)$$

ω_{nm} is the angular velocity of the oscillating σ_{nm} coherence, with an exponential decay due to transverse relaxation (T_{2nm}); the damping term of the coherences have been omitted in Table II for convenience, since it does not contain frequency information. It can be seen from Table II that the second pulse can create ZQC (and MQC) and that these elements can now be nonzero and can evolve during the evolution period, t_1, each at their appropriate ZQT (or MQT) frequencies. Since the signal observable during

(14) Kaplan, J. I.; Meiboom, S. *Phys. Rev.* **1957**, *106*, 499.
(15) Yatsiv, S. *Phys. Rev.* **1958**, *113* 1522.
(16) Schaublin, S.; Hoehner, A.; Ernst, R. R. *J. Magn. Reson.* **1974**, *13*, 196.
(17) The first two pulses in Figure 1 are necessary to "excite" or create ZQC.
(18) (a) Maudsley, A. A.; Wokaun, A.; Ernst, R. R. *Chem. Phys. Lett.* **1978**, *55*, 9. (b) Following a referee's question we make a distinction between ZQT (MQT) and ZQC (MQC). This distinction can be understood on the basis of a "conventional" spectrum where the one quantum transition 1,2 (for instance) is made of the difference ($\sigma_{12} - \sigma_{21}$) between the one quantum coherences σ_{12} and σ_{21} when detection is done by using a single coil along the y axis.
(19) Vega, S.; Pines, A. *J. Chem. Phys.* **1977**, *66*, 5624.
(20) Hatanaka, H.; Terao, T.; Hashi, T. *J. Phys. Soc. Jpn.*, **1975**, *39*, 835.
(21) Stoll, M. E.; Vega, A. J.; Waughan, R. W. *J. Chem. Phys.* **1977**, *67*, 2029.

Table III. Energy Levels and ZQT Frequencies for an ABC System

M	level	energy[a]	ZQT	frequency
−3/2	8 − − −	$(f_A + f_B + f_C)/2 + (J_{AB} + J_{AC} + J_{BC})/4$		
−1/2	7 − − +	$(f_A + f_B + f_C)/2 + (J_{AB} - J_{AC} - J_{BC})/4$	$(A^-)B^+C^-$: 6 → 7	$(f_B - f_C) - (J_{AB} - J_{AC})/2$
	6 − + −	$(f_A - f_B + f_C)/2 - (J_{AB} - J_{AC} + J_{BC})/4$	$A^+(B^-)C^-$: 5 → 7	$(f_A - f_C) - (J_{AB} - J_{BC})/2$
	5 + − −	$-(f_A - f_B - f_C)/2 - (J_{AB} + J_{AC} - J_{BC})/4$	$A^+B^+(C^-)$: 5 → 6	$(f_A - f_B) - (J_{AC} - J_{BC})/2$
+1/2	4 − + +	$(f_A - f_B - f_C)/2 - (J_{AB} + J_{AC} - J_{BC})/4$	$A^+B^-(C^+)$: 3 → 4	$(f_A - f_B) + (J_{AC} - J_{BC})/2$
	3 + − +	$-(f_A - f_B + f_C)/2 + (J_{AB} - J_{AC} + J_{BC})/4$	$A^+(B^+)C^-$: 2 → 4	$(f_A - f_C) + (J_{AB} - J_{BC})/2$
	2 + + −	$-(f_A + f_B - f_C)/2 + (J_{AB} - J_{AC} - J_{BC})/4$	$(A^+)B^+C^-$: 2 → 3	$(f_B - f_C) + (J_{AB} - J_{AC})/2$
+3/2	1 + + +	$-(f_A + f_B + f_C)/2 + (J_{AB} + J_{AC} + J_{BC})/4$		

[a] Expressed in frequency units.

the detection period (t_2) can arise only from the single quantum coherences (eq 3), it is necessary to transfer the ZQC (or MQC) information into these elements by a third (mixing) pulse. This can be seen in the final expression for the $[\sigma_{12}]_{t_2}$ element in Table II, which contains terms of the type

$$a(\tau)b(t_1)\exp(-i\omega_{12}t_2)$$

The amplitude of each line in the final 2D spectrum will be governed by the function $a(\tau)$, which is critical for the practical applications of this experiment. The function $b(t_1)$ will contain terms involving zero, single, and multiple quantum transition frequencies and will show a *complex* amplitude modulation of the detected signal as a function of t_1. The form of $[\sigma]_{t_2}$ indicates that a double Fourier transformation with respect to t_2 and t_1 will show only the observable SQT in the f_2 domain while the f_1 domain includes, in addition, all "forbidden" transitions. Thus the τ domain (preparation period) and the t_1 domain (evolution period) respectively influence the amplitudes and frequencies of the n-quantum transitions studied by a 2D NMR experiment. The present work deals specifically with the ZQT spectral analysis (i.e., the f_1 domain) and will be discussed for weakly coupled AB, ABC, AB_2, ABCD, and AB_3 spin systems.

Spectral Analysis of Zero Quantum Transitions

Generalization. ABCD... refers to a weakly coupled spin $^1/_2$ system having energies $f_A, f_B, \ldots$ ($f_A > f_B > \ldots$ is assumed), respectively, expressed in frequency units with respect to the transmitter frequency, and coupling constants $J_{AB}, J_{AC}, \ldots$.

The basic product functions and corresponding energy levels are described in standard NMR texts,[22,23] usually in the context of analysis for the allowed single quantum transitions. These basic analyses are easily extended to predict the frequencies of the ZQT spectra. The "selection rule" for ZQT is $\Delta M = 0$, where M is the projection of the total spin angular momentum in the z direction. Spin functions will be represented by standard + and − symbols in nondegenerate systems (α and β will be used in the case of degeneracy).

It has already been noted by Wokaun and Ernst[9] that different types of ZQT can be defined, depending on whether one or several pairs of spins are involved in a transition for which $\Delta M = 0$. For the purpose of the present discussion, the terms "transition of the *first-kind*" will refer to the ZQT involving only one pair of spins (the other spins being unchanged), ZQT of the *second-kind* will refer to a change of two pairs of spins, and so on. The following transition notation, which is convenient for predicting the frequencies involved, is also introduced; for example, a transition of the first kind in an ABCD system,

$$+-++ \rightarrow ++-+$$

will be denoted by $(A^+)B^-C^+(D^+)$, where the parentheses around the A and D nuclei imply that the + spins corresponding to these nuclei remain unchanged, while the B and C spins, which are involved in the transition, change from − to + and + to −, respectively. The signs in the above notation refer to the initial states, and the notation is limited to nonequivalent spins.[24]

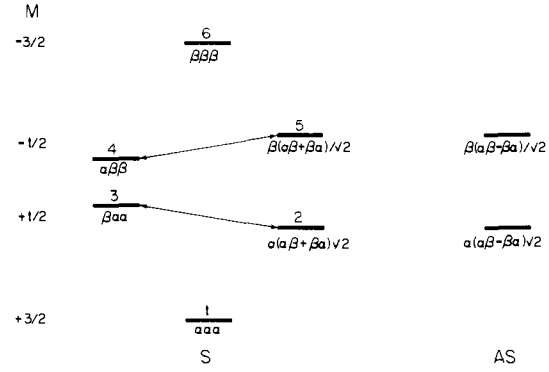

Figure 2. Energy level representation for an AB_2 spin $^1/_2$ system; S and AS refer to the symmetric and antisymmetric functions, respectively. The possible ZQT's are indicated by the arrows.

AB System. This is the simplest case of a coupled spin $^1/_2$ system which will be expected to show a single ZQT, as can be seen in Table I. Since ZQT appear as a complex amplitude modulation of the NMR observable (i.e., SQC in the density matrix), the frequencies corresponding to both 2 → 3, A^+B^-, and 3 → 2, B^+A^- (opposite in sign), are expected in the ZQT spectrum, but for convenience only the positive (absolute) frequencies will be presented in the following discussions. The ZQT, A^+B^-, in this example will appear with the frequency $(f_A - f_B)$ and is independent of J_{AB}. It can be noted from Table I that the double quantum transition (DQT) appearing at $(f_A + f_B)$ corresponds to a higher frequency than the ZQT. In this simple case, the ZQT spectrum will not provide more information than the conventional SQT spectrum.

ABC System. Table III gives the energy levels for the ABC system and the possible ZQT frequencies, which are centered at the chemical shift difference between each pair of nuclei. The ZQT spectrum will show three doublets centered at $(f_A - f_B)$, $(f_A - f_C)$, and $(f_B - f_C)$, the splittings being $|(J_{AC} - J_{BC})|$, $|(J_{AB} - J_{BC})|$, and $|(J_{AB} - J_{AC})|$, respectively. Inspection of these ZQT frequencies will indicate that the chemical shift difference between two nuclei, for example, A and B, is associated with the coupling constants J_{AC} and J_{BC} but not their mutual coupling, J_{AB}. This feature is quite general to ZQT's of the first kind and can be easily extended to other systems which show multiplets of the form

$$(f_A - f_B) \pm (J_{AC} - J_{BC}) \pm (J_{AD} - J_{BD}) \pm \ldots$$

The appearance of chemical shift and coupling constant *differences* in ZQT spectra is very different from conventional NMR spectroscopy, and it is this feature which provides a technique for correlating chemical shifts and coupling constants. Because the coupling constant terms appear as *differences*, their relative signs have significance in the ZQT spectra and hence can be evaluated by intercomparison between the normal (SQT) and ZQT spectra.

(22) Emsley, J. W.; Feeney, J.; Sutcliff, L. H. "High Resolution Nuclear Magnetic Resonance Spectroscopy"; Pergamon Press: London, 1966; Vol. I.
(23) Pople, J. A.; Schneider, W. G.; Bernstein, J. "High Resolution Nuclear Magnetic Resonance"; McGraw-Hill: New York, 1969.

(24) It is interesting to note that although for molecules in isotropic solution ZQT's occur only between levels belonging to the same irreducible representation, Tang and Pines have recently demonstrated how this rule can be broken in the case of an "oriented" CH_3 group.[25] Also, when degenerated levels are present, it is better to use basic spin functions belonging to the irreducible representations of the corresponding group of symmetry which renders the nomenclature used no longer applicable as indicated in Table V.
(25) Tang, J.; Pines, A. *J. Chem. Phys.* **1980**, *72*, 3290.

Table IV. Energy Levels for an ABCD System, Expressed in Frequency Units

M	level	energy
−2	16 − − − −	$(f_A + f_B + f_C + f_D)/2 + (J_{AB} + J_{AC} + J_{AD} + J_{BC} + J_{BD} + J_{CD})/4$
	15 − − − +	$(f_A + f_B + f_C - f_D)/2 + (J_{AB} + J_{AC} - J_{AD} + J_{BC} - J_{BD} - J_{CD})/4$
	14 − − + −	$(f_A + f_B - f_C + f_D)/2 + (J_{AB} - J_{AC} + J_{AD} - J_{BC} + J_{BD} - J_{CD})/4$
−1	13 − + − −	$(f_A - f_B + f_C + f_D)/2 - (J_{AB} - J_{AC} - J_{AD} + J_{BC} + J_{BD} - J_{CD})/4$
	12 + − − −	$-(f_A - f_B - f_C - f_D)/2 - (J_{AB} + J_{AC} + J_{AD} - J_{BC} - J_{BD} - J_{CD})/4$
	11 − − + +	$(f_A + f_B - f_C - f_D)/2 + (J_{AB} - J_{AC} - J_{AD} - J_{BC} - J_{BD} + J_{CD})/4$
	10 − + − +	$(f_A - f_B + f_C - f_D)/2 - (J_{AB} - J_{AC} + J_{AD} + J_{BC} - J_{BD} + J_{CD})/4$
	9 − + + −	$(f_A - f_B - f_C + f_D)/2 - (J_{AB} + J_{AC} - J_{AD} - J_{BC} + J_{BD} + J_{CD})/4$
0	8 + − − +	$-(f_A - f_B - f_C + f_D)/2 - (J_{AB} + J_{AC} - J_{AD} - J_{BC} + J_{BD} + J_{CD})/4$
	7 + − + −	$-(f_A - f_B + f_C + f_D)/2 - (J_{AB} - J_{AC} + J_{AD} + J_{BC} - J_{BD} + J_{CD})/4$
	6 + + − −	$-(f_A + f_B - f_C - f_D)/2 + (J_{AB} - J_{AC} - J_{AD} - J_{BC} - J_{BD} + J_{CD})/4$
	5 − + + +	$(f_A - f_B - f_C - f_D)/2 - (J_{AB} + J_{AC} + J_{AD} - J_{BC} - J_{BD} - J_{CD})/4$
	4 + − + +	$-(f_A - f_B + f_C + f_D)/2 - (J_{AB} - J_{AC} - J_{AD} + J_{BC} + J_{BD} - J_{CD})/4$
+1	3 + + − +	$-(f_A + f_B - f_C + f_D)/2 + (J_{AB} - J_{AC} + J_{AD} - J_{BC} + J_{BD} - J_{CD})/4$
	2 + + + −	$-(f_A + f_B - f_C + f_D)/2 + (J_{AB} + J_{AC} - J_{AD} + J_{BC} - J_{BD} - J_{CD})/4$
+2	1 + + + +	$-(f_A + f_B + f_C + f_D)/2 + (J_{AB} + J_{AC} + J_{AD} + J_{BC} + J_{BD} + J_{CD})/4$

ZQT Frequencies for an ABCD Case

transitions of the first kind	transitions of the second kind
$(f_A - f_B) \pm \frac{1}{2}\{(J_{AC} - J_{BC}) \pm (J_{AD} - J_{BD})\}$	$(f_A - f_B) + (f_C - f_D)$
$(f_A - f_C) \pm \frac{1}{2}\{(J_{AB} - J_{BC}) \pm (J_{AD} - J_{CD})\}$	$(f_A - f_C) + (f_B - f_D)$
$(f_A - f_D) \pm \frac{1}{2}\{(J_{AB} - J_{BD}) \pm (J_{AC} - J_{CD})\}$	$(f_A - f_D) + (f_B - f_C)$
$(f_B - f_C) \pm \frac{1}{2}\{(J_{AB} - J_{AC}) \pm (J_{BD} - J_{CD})\}$	
$(f_B - f_D) \pm \frac{1}{2}\{(J_{AB} - J_{AD}) \pm (J_{BC} - J_{CD})\}$	
$(f_C - f_D) \pm \frac{1}{2}\{(J_{AC} - J_{AD}) \pm (J_{BC} - J_{BD})\}$	

The AB_2 system is a special case of a three-spin system, and the corresponding energy levels are given in Figure 2, in which the functions of nuclei B are separated according to their symmetry. ZQT's will be expected only within each of the $M = \pm^1/_2$ submanifolds and, since elements of different symmetry do not mix in the density matrix, only elements belonging to the same irreducible representation within a given M submanifold will give rise to ZQT lines. Therefore in this case we would expect the ZQT's 2 → 3 and 4 → 5 at frequencies $(f_A - f_B) \pm {}^1/_2 J_{AB}$. Note that the coupling J_{AB} appears in the above term but not J_{BB}.

ABCD System. Table IV gives the levels and their corresponding energies, in frequency units, for an ABCD case, including all possible ZQT frequencies. If we first consider the transitions within the $M = +1$ submanifold, six ZQT's are expected (due to the six possible chemical shift differences), each of the form

$$(f_C - f_D) + \tfrac{1}{2}[(J_{AC} - J_{AD}) + (J_{BC} - J_{BD})] \qquad (A^+)(B^+)C^+D^-: 2 \rightarrow 3$$

The corresponding transitions in the $M = -1$ submanifold will be of the form

$$(f_C - f_D) - \tfrac{1}{2}[(J_{AC} - J_{AD}) + (J_{BC} - J_{BD})] \qquad (A^-)(B^-)C^+D^-: 14 \rightarrow 15$$

Taken together, these 12 transitions correspond to the six doublets in the ZQT spectrum (only positive frequencies being considered), arising from the $M = \pm 1$ levels.

Similarly one can expect 15 ZQT's arising from the $M = 0$ level; of these, three are ZQT's of the second kind, involving the simultaneous change to two pairs of spins, namely, $A^+B^+C^-D^-$, $A^+B^-C^+D^-$, and $A^+B^-C^-D^+$, and occurring at frequencies $(f_A - f_B) + (f_C - f_D)$, $(f_A - f_C) + (f_B - f_D)$, and $(F_A - f_D) + (f_B - f_C)$; note that these transitions appear at relatively higher frequencies and are singlets. The remaining 12 ZQT's are of the first kind, and the transitions involving the chemical shift differences, for example, between C and D nuclei, will be of the form

$$(f_C - f_D) + \tfrac{1}{2}[(J_{AC} - J_{AD}) - (J_{BC} - J_{BD})] \qquad (A^+)(B^-)C^+D^-: 7 \rightarrow 8$$

$$(f_C - f_D) - \tfrac{1}{2}[(J_{AC} - J_{AD}) - (J_{BC} - J_{BD})] \qquad (A^-)(B^+)C^+D^-: 9 \rightarrow 10$$

Thus the final ZQT spectrum will contain 27 lines (Table IV), composed of six quartets (doublets of doublets), one centered at each of the six possible frequency differences $\Delta_{AB}, \ldots$, with the splitting pattern $\pm(J_{AC} - J_{BC}) \pm (J_{AD} - J_{BD}), \ldots$ and three singlets corresponding to the ZQT's of the second kind. (Note that the corresponding SQT spectrum consists of 56 transitions, 24 of which are combination lines.)

Another four-spin system of interest is the AB_3 case; three of the nuclei are equivalent and hence the B_3 subsystem may be represented according to the C_3 symmetry group. the basic symmetry functions may be classified with respect to the A_1 or E irreducible representations as shown in Table V (the subscripts refer to the M values). The ZQT's originating from the various levels are indicated in Table VI. The ZQT spectrum will show signals at frequencies $(f_A - f_B) \pm J_{AB}$ and $(f_A - f_B)$.[24]

The above discussions can be easily extended to more complicated spin systems to predict the ZQT spectra by following procedures similar to those of conventional NMR spectral analysis. First, the stationary state wave functions should be determined and their energies calculated; then the frequencies of the ZQT's can be predicted by considering only the transitions between states of a given M submanifold ($\Delta M = 0$) and function of same symmetry, as discussed earlier.

Table V. Energies and Basic (symmetry) Functions Corresponding to an AB_3 System[a]

state	basic function	energy[b]
A_{-2}	$\beta\beta\beta$	$(f_A + 3f_B)/2 + 3J/4$
$1A_{-1}$	$\beta\{\beta\beta\alpha + \beta\alpha\beta + \alpha\beta\beta\}/\sqrt{3}$	$(f_A + f_B)/2 + J/4$
$2A_{-1}$	$\alpha\beta\beta\beta$	$-(f_A - 3f_B)/2 - 3J/4$
$1A_0$	$\beta\{\alpha\alpha\beta + \alpha\beta\alpha + \beta\alpha\alpha\}/\sqrt{3}$	$(f_A - f_B)/2 - J/4$
$2A_0$	$\alpha\{\beta\beta\alpha + \beta\alpha\beta + \alpha\beta\beta\}/\sqrt{3}$	$-(f_A - f_B)/2 - J/4$
$1A_1$	$\beta\alpha\alpha\alpha$	$(f_A - 3f_B)/2 - 3J/4$
$2A_1$	$\alpha\{\alpha\alpha\beta + \alpha\beta\alpha + \beta\alpha\alpha\}/\sqrt{3}$	$-(f_A + f_B)/2 + J/4$
A_2	$\alpha\alpha\alpha\alpha$	$-(f_A + 3f_B)/2 + 3J/4$
E_{-1}	$\beta\{\beta\beta\alpha - \beta\alpha\beta\}/\sqrt{2}$	$(f_A + f_B)/2 + J/4$
$1E_0$	$\beta\{\alpha\alpha\beta - \alpha\beta\alpha\}/\sqrt{2}$	$(f_A - f_B)/2 - J/4$
$2E_0$	$\alpha\{\beta\beta\alpha - \beta\alpha\beta\}/\sqrt{2}$	$-(f_A - f_B)/2 - J/4$
E_1	$\alpha\{\alpha\alpha\beta - \alpha\beta\alpha\}/\sqrt{2}$	$-(f_A + f_B)/2 + J/4$

[a] The A and E states of the C_3 symmetry group are indicated in the left-hand column; the subscripts here indicate the M values. The E states are doubly degenerate but only one of the functions is represented. [b] J refers to J_{AB}.

Table VI. ZQT's and Their Energies Given in Frequency Units for an AB_3 Case (See Table V)

ZQT	energy
$2A_1 \rightarrow 1A_1$	$(f_A - f_B) - J_{AB}$
$2A_0 \rightarrow 1A_0$	$(f_A - f_B)$
$2A_{-1} \rightarrow 1A_{-1}$	$(f_A - f_B) + J_{AB}$
$2E_0 \rightarrow 1E_0$	$(f_A - f_B)$

Applications of ZQT Spectroscopy in Chemistry

It might have been anticipated that explicit analysis of the ZQT spectrum of the multiple spin system of a typical, complex organic

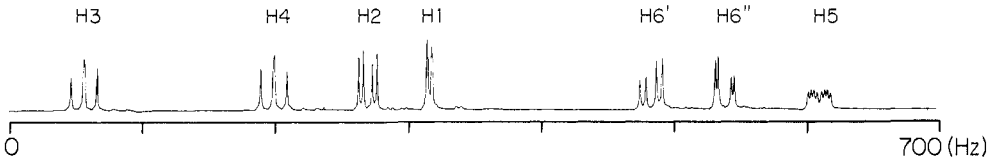

Figure 3. The normal 270-MHz FT NMR spectrum of trideuteriomethyl 2,3,4,6-tetra-*O*-trideuteriomethyl-α-D-glucopyranoside (**1**) in benzene-d_6 (0.1 M). The scale represents the offset from the transmitter frequency.

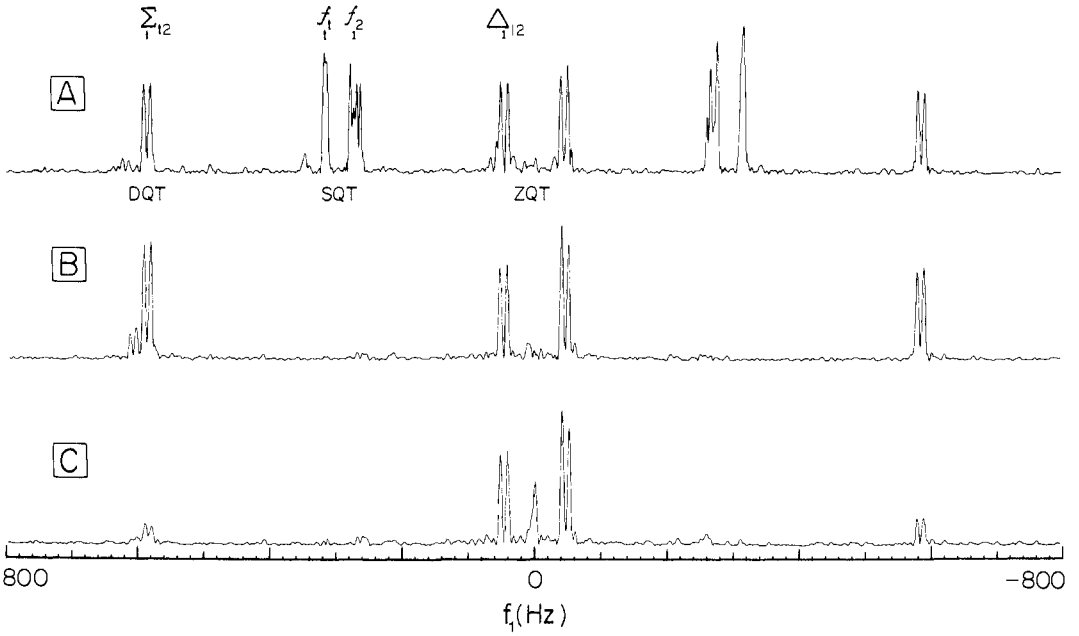

Figure 4. Trace A was obtained using the basic pulse sequence $90_\phi° - \tau - 90_\phi° - t_1 - 90° -$ acquisition (τ = 200 ms, ϕ = 0°) and represents the f_1 domain corresponding to the H1 proton. Trace B shows the selective suppression of the SQT's, achieved by shifting the phase of the two initial pulses by 180°. The DQT were suppressed, as seen in trace C, by co-adding signals from two separate experiments in which the initial pulses were phase shifted from 90 to 270°. The incomplete cancellations are probably due to pulse (phase) imperfections and long-term instabilities (see Experimental Section). Note added in proof: the spectrometer is now controlled by a Nicolet 293 B pulse programmer, using the NTCFTB software. As a result it is now possible to alter the phase shift during a single, integrated experiment, which leads to substantially better suppression of the DQT.

molecule would be both cumbersome and time consuming. However, it will be noted from the above formalism that since ZQC can only be created between spins which have mutual spin–spin coupling, a type of subspectral analysis is invariably possible—long-range couplings (across four, or more, bonds) are frequently of small or zero magnitude and so it is generally possible to consider *in isolation* only those spins which have a vicinal or geminal coupling; as will be seen, this substantially simplifies analysis of ZQT spectra in practical cases. We shall illustrate this point, and hence some of the diagnostic potential of ZQT spectroscopy in organic chemistry, by a study of trideuteriomethyl 2,3,4,6-tetra-*O*-trideuterioacetyl-α-D-glucopyranoside (**1**), which is a seven-spin system (Figure 3; Table VII).

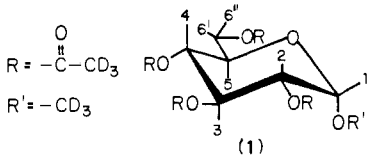

The 2D spectrum resulting from the three-pulse experiment (Figure 1) described earlier will contain the conventional SQT frequencies in the f_2 domain and all possible n-quantum transition frequencies in the f_1 domain. However, by use of suitable phase-shifted sequences it is possible to selectively observe only the ZQT spectrum (in f_1).[8] This point is illustrated in Figure 4 which shows transitions, corresponding to the H1 proton (in f_2). Spectrum A is an f_1 trace obtained using the basic pulse sequence (ϕ = 0°) and shows the responses due to zero, single, and multiple (double) quantum transitions. Figure 4B shows that phase shifting the two excitation pulses by 180° (e.g., ϕ = 90 and 270°) results in cancellation of the SQT's (odd n-quantum transitions) while retaining the zero and double (even n-) quantum transitions in the final spectrum. Suppression of the double quantum transitions can be obtained by shifting the pulse phase ϕ by 0, 90, and 180, and 270° and is shown in Figure 4C;[26] in this case it leads to the detection of the ZQT spectrum.

Table VII. Conventional and ZQT Spectral Data for Trideuteriomethyl 2,3,4,6-Tetra-*O*-(trideuterioacetyl)-α-D-glucopyranoside (1)

frequency,[a] Hz	coupling constants,[b] Hz	shift separations,[c] Hz	ZQT results,[d] Hz
$f_1 = 316$	$J_{12} = 3.8$	$\Delta_{12} = 41$	$J_{12} = 4$
$f_2 = 275$	$J_{23} = 10.6$	$\Delta_{23} = 219$	$J_{23} = 10.5$
$f_3 = 56$	$J_{34} = 9.5$	$\Delta_{34} = 144$	$J_{34} = 9.5$
$f_4 = 200$	$J_{45} = 10.6$	$\Delta_{45} = 411$	$J_{45} = 10.5$
$f_5 = 611$	$J_{56'} = 4.7$	$\Delta_{56'} = 127$	$\lvert(J_{56'} - J_{6'6''})\rvert = 16.5$
$f_{6'} = 484$	$J_{56''} = 2.5$	$\Delta_{56''} = 72$	$\lvert(J_{56''} - J_{6'6''})\rvert = 14$
$f_{6''} = 539$	$J_{6'6''} = 12.5$	$\Delta_{6'6''} = 55$	$\lvert(J_{56'} - J_{56''})\rvert = \sim 2$[e]

[a] Offset from the transmitter frequency. [b] From ref 30. [c] The chemical shift differences obtained from the conventional spectrum; a direct comparison of these separations between the protons can be made by matching the conventional spectrum with the ZQT traces (e.g., $(f_1 - f_2)$ in Figure 3 is equal to the separation between the Δ_{23} multiplets in Figure 5B). [d] Obtained from ZQT spectra with 1.5-Hz digital resolution. [e] Not well resolved because of limited resolution and overlap (see Figure 5C).

(26) In this instance, trace C in Figure 4A was obtained by adding the time domain signals (interferrograms) from two separate experiments (ϕ = 0, 180° and 90, 270°); however, it would be preferable to effect the same within a single, composite experiment.

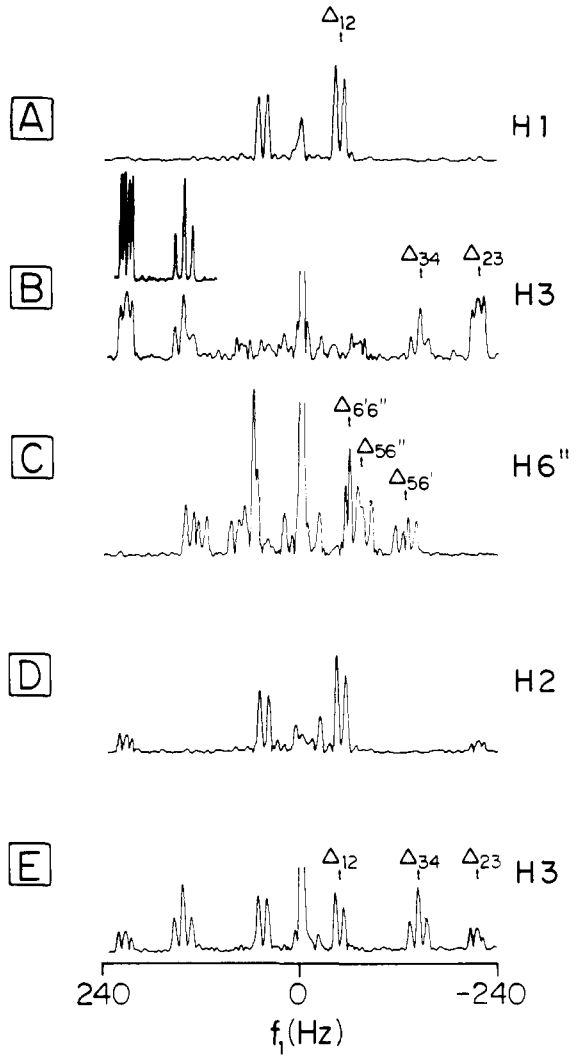

Figure 5. ZQT (absolute value) spectra for the protons indicated, each corresponding to a single trace in f_1. The appropriate " interferrograms" (512 × 2 words) were zero-filled, and apodized to improve the effective resolution. The trace shown as an inset was obtained for H3 by halving the f_1 width to achieve higher digital resolution. The experimental parameters were: digitization in f_2, 0.68 Hz; increment in t_1, 625 μs; number of acquisitions, 8; preparation delay (τ), 200 ms (except trace B, 260 ms).

The ZQT spectrum corresponding to the H1 proton[27] gives a simple pattern because H1 is coupled to only one other proton, H2 (J_{12} = 3.8 Hz). The ZQT spectrum is expected to show a multiplet centered at the chemical shift difference $\pm(f_1 - f_2)$ (which is denoted by Δ_{12}). The structure of this multiplet can be predicted by considering these transitions as arising from an ABC "subspin system" (see Table III), involving H1, H2, and H3:

$$\Delta_{12} \pm \tfrac{1}{2}(J_{13} - J_{23})$$

The multiplet is observed as a doublet, separated by J_{23} = 10.6 Hz; the transitions corresponding to Δ_{13} do not appear in the ZQT spectrum since there is no appreciable spin–spin coupling between H1 and H3.[29,30]

Similar arguments may be used to predict the possible ZQT's corresponding to the H3 proton. Since H3 is coupled to H2 (J = 10.5 Hz) and H4 (J = 9.5 Hz), two multiplets centered at Δ_{23} and Δ_{34} will be in the ZQT spectrum, arising from the subspin systems, H1, H2, H3, H4 and H2, H3, H4, H5, respectively. The multiplet patterns for these signals are given by (Table IV)

$$\Delta_{23} \pm \tfrac{1}{2}[(J_{12} - J_{13}) \pm (J_{24} - J_{34})] = \Delta_{23} \pm \tfrac{1}{2}(J_{12} \pm J_{34})$$

and

$$\Delta_{34} \pm \tfrac{1}{2}[(J_{23} - J_{24})(J_{35} - J_{45})] = \Delta_{34} \pm \tfrac{1}{2}(J_{23} \pm J_{45})$$

These multiplets are illustrated in the ZQT traces in Figure 5B. The above examples demonstrate a potential use for ZQT spectra in structural analysis, namely for establishing connectivities between weakly coupled protons. In addition, the splitting patterns provide a method for indirectly obtaining coupling constants; for example, it should be possible, in principle, to determine the coupling constants J_{12}, J_{45} by analyzing the ZQT spectrum of H3 (J_{34} and J_{23} will appear in the f_2 domain, corresponding to the conventional SQT's).

The H6" proton is part of the H6', H6", H5, H4 subspin system, and is coupled to H6' (J = 12.5 Hz) and H5 (J = 2.5 Hz). Following the earlier discussion the ZQT spectrum corresponding to the H6" proton would be expected to show the signals

$$\Delta_{56''} \pm \tfrac{1}{2}[(J_{45} - J_{46''}) \pm (J_{56'} - J_{6'6''})] = \Delta_{56''} \pm \tfrac{1}{2}[(J_{45}) \pm (J_{56'} - J_{6'6''})]$$

and

$$\Delta_{6'6''} \pm \tfrac{1}{2}(J_{56'} - J_{56''})$$

In addition to these chemical shift differences, another multiplet centered at $\Delta_{56'}$ is seen in Figure 5C with the frequency pattern

$$\Delta_{56'} \pm \tfrac{1}{2}[(J_{45} - J_{46'}) \pm (J_{56''} - J_{6'6''})] = \Delta_{56'} \pm \tfrac{1}{2}[(J_{45}) \pm (J_{56''} - J_{6'6''})]$$

This multiplet, unlike in the previous examples, would be expected when observing H6" since there is a finite coupling ($J_{56'}$ = 4.7 Hz) between H5 and H6' protons, which are also coupled to H6".

An interesting feature in the ZQT spectrum of H6" is the appearance of the geminal (negative) coupling $J_{6'6''}$, as a *difference*. This enables the distinction to be made between positive and negative coupling constants,[31] which is rarely used in conventional spectral analysis mainly because of the difficulty in obtaining this information. This could help in distinguishing between the geminal (negative) and trans-diaxial (positive) couplings of steroids, which are of similar magnitude.[32]

The delay times τ (200, 260, and 200 ms, respectively) used to obtain the ZQT spectra shown in Figure 5A, B, and C were selected to give optimum signal intensities to illustrate the expected spectral patterns. However, it should be noted that the ZQT signal intensity is a rather complicated function of both coupling constants and chemical shift frequencies, which makes it difficult to *simultaneously optimize* conditions for all protons in the spectrum. For example, the ZQT spectra (Figure 5D and E) corresponding to the H2 and H3 protons for τ = 200 ms show relatively weak signals for the multiplet Δ_{23} (cf. trace B), indicating the significance of the preparatory delay in these experiments for optimum signal intensities. Although in all the previous discussions only the protons with vicinal or geminal relationship were considered, Figure 5E, which corresponds to the H3 proton, shows a doublet at Δ_{12}; this reflects the fact that H3 is indirectly connected to H1 via H2. Such responses from the indirectly connected protons were generally found to be weak in the present study and hence they have not been emphasized. (This should be compared with

(27) "*ZQT spectrum of the H1 proton*", refers to the (ZQT) traces in the F_1 domain corresponding to the of frequencies in f_2. The ZQT spectrum may be obtained as a single trace from the 2D spectrum or an integral projection[28] of the selected (H1) region onto f_1.

(28) Muller, L.; Kumar, A.; Ernst, R. R. *J. Chem. Phys.* **1976**, *63*, 5490.

(29) Long-range, four-bond couplings (ca. <0.8 Hz) can be detected in these type of molecules between 1,3-axial, equatorial protons;[30] however, the choice of the preparation delay τ (~200–300 ms) is generally too short to allow for any significant contribution from protons more than three bonds away. The limited digital resolution and line-broadening in f_2 further decrease the detection of the ZQT's associated with these couplings.

(30) Hall, L. D.; Sukumar, S.; Sullivan, G. R. *J. Chem. Soc., Chem. Commun.* **1979**, *N6*, 292.

(31) For example, the multiplet at $\Delta_{56'}$ shows two large couplings of about 10 and 14 Hz, the latter arising from the J difference [2.5 - (-12.5)1.

(32) Hall, L. D.; Sanders, J.K.M. *J. Am. Chem. Soc.* **1980**, *102*, 5703.

the earlier discussion on the (absence of) signals at Δ_{13} due to small long-range couplings.[29])

Although we have deliberately chosen a weakly coupled multispin system, with relatively simple subspin systems, it is evident from Table IV that ZQT of the second kind could well give rise to additional peaks for more complicated spin systems. In general these lines may be expected to appear at relatively higher frequencies in f_1 than those of the first kind and they should, therefore, be easily identified.

Conclusion

It is evident from previous studies on the analysis of complex proton NMR spectra that versatile, new techniques for assigning proton resonances are necessary to complement the high resolving power of proton 2D J spectroscopy. One such technique is ^{13}C-{^1H} chemical shift correlation spectroscopy.[33,34] Providing that the ^{13}C spectrum has been assigned, this provides a direct and unequivocal assignment for all the directly bonded protons; one minor disadvantage is that sufficient material is required for a ^{13}C NMR experiment. The equivalent homonuclear experiments have also been reported.[2,3,12,13] The connectivity information obtained from either of these correlation experiments is analogous to that which could be obtained by conventional, multiple resonance experiments;[35] however, the 2D methods have the main advantage of providing this information from a "single" experiment, without limitations imposed by lack of selectivity of the irradiating frequencies, which is particularly important when dealing with closely spaced or overlapping resonances.

The use of ZQT spectra to obtain connectivities appears to have the following advantages over the homonuclear (^1H) shift correlation methods.

(a) The ZQT's are independent of field inhomogeneity, enabling one to obtain high resolution spectra (in f_1) which are limited mainly by "natural" line widths (cf. J spectra[36]).

(b) The transition frequencies (of the first kind) appear as chemical shift *differences*, which may considerably reduce the spectral width in the f_1 domain; this has a number of practical advantages. Since the size of the data matrix can now be reduced to achieve the suitable digitization in the final 2D spectrum (cf. ref 3, 12, and 13), this could in turn lead to significant time saving in data acquisition and processing, and also minimize the problems associated with the handling of large data arrays.

(c) It should be possible, as described in the previous section, to indirectly determine the relative signs of coupling constants.

(d) ZQT spectra generally exhibit fewer lines than the corresponding SQT spectra, which could help simplify spectral analysis.

(e) It is known that in 2D correlation spectroscopy there is no net magnetization transfer[33,34,37] and that it results in multiplets which have both positive- and negative-going signals; it is conceivable that limited digital resolution in either dimension could result in cancellation of these signals.[33] However, in spite of the limited digital resolution used to obtain the traces in Figure 5, all ZQT's show finite intensities (this point will be discussed further elsewhere).[38]

Since ZQT's are independent of magnetic field inhomogeneity effects, the higher order n-quantum transitions may be eliminated by applying a field gradient pulse during the evolution period,[9] thereby obviating the need for elaborate phase-cycling procedures. On the other hand, if one needs to selectively study, for example, SQT's or DQT's, it is only necessary to add or subtract signals resulting from the appropriate phase shifting of the excitation pulse. In this context it should be noted that errors in pulse-phase and -flip angle can contribute to inperfections in the experimental data; Bodenhausen et al.[10] have described phase-cycling procedures to minimize these effects, and also those arising from (T_1) relaxation during the experiment.

Although DQT's also contain connectivity information, the relatively higher frequencies in f_1 (sums of chemical shifts) and the greater sensitivity to field inhomogeneity effects make DQT spectra less desirable for practical applications.

A potential limitation of ZQT spectroscopy is the dependence of the *intensity* of the signals in the final 2D spectrum on the preparation delay, τ. For example, it was necessary in this study of **1** to perform several individual experiments to select suitable values of τ to maximize ZQT signal intensities, and thus obtain high resolution information. On the other hand, it may be that this τ dependence of signal intensities can be used to simplify ZQT spectra by reducing the total number of lines in a complex 2D spectrum. In either event it will be necessary to have more experience of the experimental practice of ZQT spectroscopy and a deeper theoretical understanding of the signal intensity dependencies; both of these are under active consideration.

Experimental Section

The spectrometer used in this study was assembled at U.B.C. from components which originally comprised a Nicolet TT-23 console, and a superconducting solenoid (6.3 T) from Oxford Instruments. In its present configuration, the instrument is controlled by a Nicolet 1180 computer (40K) driving a Nicolet 293A′ pulse controller; data were acquired using the standard NTC FT program and were stored and processed on two disk drives (Diablo, Series 30) each with a one megaword disk.

As noted before, in this case the cancellation of the odd n-quantum transitions was effected by using the following sequence ($\phi = 0°$): (1) initial pulse with a phase shift ϕ^0, (2) preparation delay (τ), (3) second pulse with (ϕ^0) phase shift, (4) incremental delay (t_1), (5) third (mixing) pulse with 0° phase, (6) signal acquisition, (7) relaxation delay, (8) repeat sequence 1 to 7 with $\phi = (\phi + 180)°$ phase shift, (9) signal average by repeating sequence 1 through 8.

The selective detection of ZQT's (Figures 4 and 5) was achieved by adding the time-domain signals (interferrograms) from a separate experiment, similar to the sequence 1 to 9, but with ϕ being equal to 90°.

The signals $S(t_1,t_2)$ were acquired on 2048-word size blocks, for 512 increments (625 μs) in t_1. After the first Fourier transformation with respect to t_2 and transposition, individual "interferrograms" were zero-filled and Fourier transformed with respect to t_1, to give the traces, $S(f_2,f_1)$ shown in Figures 4 and 5. The preparation delay τ was set to ca. 100–300 ms (which is of the order of the inverse, average coupling constant) for optimum signal intensities in the final spectrum.

Acknowledgment. This work was supported by operating grants from the National Research Council of Canada (A1905 to L. D.H.). It is a pleasure to thank U.B.C. for the award of a Graduate Research Studentship (to S.S.). One of us (G.P.) thanks the French Ministries of University and Foreign Affairs for allowing his stay at U.B.C.

(33) Bodenhausen, G.; Freeman, R. *J. Magn. Reson.* **1977**, *28*, 471.
(34) Freeman, R.; Morris, G. A.; *Bull. Magn. Reson.* **1979**, *1*, 5.
(35) Hoffman, R. A.; Forsen, S. "Progress in NMR Spectroscopy", Emsley, J. W.; Feeney, J.; Sutcliffe, L. H., Eds.; Pergamon Press: London, 1969; Vol. 1, Chapter 2.
(36) Freeman, R.; Hill, H. W. *J. Chem. Phys.* **1971**, *54*, 301.
(37) Maudsley, A. A.; Ernst, R. R. *Chem. Phys. Lett.* **1977**, *50*, 368.
(38) Hall, L. D.; Pouzard, G.; Sukumar, S., to be submitted for publication.